

## Synthesis of a self-assembled copper(II) metallo-rectangle with a guanosine-substituted terpyridinet

Cite this: *Dalton Trans.*, 2013, **42**, 13813

Received 9th July 2013,  
Accepted 12th August 2013

DOI: 10.1039/c3dt51845k

[www.rsc.org/dalton](http://www.rsc.org/dalton)

Sushobhan Ghosh,<sup>a</sup> Georg T. Silber,<sup>b</sup> Andrew J. P. White,<sup>a</sup> Neil Robertson<sup>\*b</sup> and Ramon Vilar<sup>\*a</sup>

**The synthesis of a terpyridine–guanosine ligand and its reaction with copper(II) to yield a new [2 + 2] metallo-rectangle is reported. The metallo-rectangle was characterized by single crystal X-ray diffraction and the structure showed significant intramolecular  $\pi$ – $\pi$  stacking interactions between the two terpyridine moieties of the molecule. This prompted us to investigate the magnetic properties of the new di-copper(II) assembly which displayed ferromagnetic interactions in the solid state.**

Self-assembly has been demonstrated to be a very efficient approach to the synthesis of complex architectures.<sup>1–6</sup> Utilizing suitable design principles one can readily synthesize discrete supermolecules from relatively simple fragments in a single step in high yields. One valuable feature of self-assembly is its dynamic nature which stems from the reversibility of non-covalent interactions. Metal coordination has proven to be a particularly useful reversible interaction for the synthesis of a plethora of supramolecular assemblies such as macrocycles, cages and helices.<sup>7–10</sup> Recent years have witnessed the rapid development of supramolecular coordination systems with potential applications in many areas including gas storage, ion-exchange, magnetism, catalysis and optoelectronics.<sup>11–16</sup> Over the past 20 years, research on molecular-based magnetism has become well established with the underlying aim of producing usable devices. Magnetic materials can be constructed to yield discrete clusters or extended structures with the magnetic moment carriers (such as paramagnetic metal ions) as the repeating unit, using appropriate bridging ligands to provide superexchange pathways between the metal centres. A number of systems have been reported in which  $\pi$ – $\pi$  stacking interactions play a major role in propagating the magnetic

properties, eventually leading to long range magnetic ordering.<sup>17–20</sup> Some of the factors that play crucial roles in transmitting strong magnetic coupling are the distance between metal centres, the nature of the bridging ligands and the spin ground state. Recently, non-covalent interactions have been exploited in the design of polymetallic magnetic materials where supramolecular interactions bring enhanced magnetic ordering in the system.<sup>21</sup>

Herein we report the synthesis of the new terpyridine–guanosine ligand **L**<sup>1</sup> (Fig. 1) and the corresponding metallo-rectangle **3** (Fig. 2). This metallo-rectangle was characterized by single crystal X-ray diffraction and the structure showed significant intra-molecular  $\pi$ – $\pi$  stacking interactions between the two terpyridine moieties of the molecule. This prompted us to investigate the magnetic properties of **3** which showed ferromagnetic interactions in the solid state.

Ligand **L**<sup>1</sup> was synthesised following the procedure outlined in Fig. 1 (see ESI† for full synthetic details). The <sup>1</sup>H NMR spectrum of **L**<sup>1</sup> indicated the absence of the N1–H proton of the guanosine moiety while other expected signals from the terpyridine and guanosine were present with the correct integration. The <sup>13</sup>C{<sup>1</sup>H} NMR spectrum was also consistent with the proposed formulation; it showed a considerable downfield shift of carbon C6 and a small downfield shift of the C8, C4, C5 and the sugar C1' carbons as compared to guanosine (see Fig. S3†). The <sup>1</sup>H–<sup>15</sup>N HMBC NMR showed the splitting of the peak at 5.5 ppm (Fig. S4†) which may be due to the non-equivalent protons present at N2 position of **L**<sup>1</sup>. The FT-IR spectrum of **L**<sup>1</sup> indicated the absence of the C=O stretching frequency in contrast to guanosine which displays a strong band at 1708 cm<sup>-1</sup>. The ESI(+) mass spectrum of this product showed a peak at 599 a.m.u. consistent with the formulation of **L**<sup>1</sup>.

The new metallo-rectangle **3** was readily synthesised by reacting **L**<sup>1</sup> with one equivalent of Cu(NO<sub>3</sub>)<sub>2</sub> in methanol (Fig. 1). This yielded a green-blue solution from which blue crystals suitable for X-ray crystallography were obtained by slow evaporation of the solvent (95% yield). The X-ray crystal structure† shows the molecule to have adopted a self-filling rectangular conformation with the central pyridyl ring of each

<sup>a</sup>Department of Chemistry, Imperial College London, South Kensington, London SW7 2AZ, UK. E-mail: [r.vilar@imperial.ac.uk](mailto:r.vilar@imperial.ac.uk)

<sup>b</sup>EaStCHEM, School of Chemistry, Joseph Black Building, West Mains Road, Edinburgh, Scotland EH9 3JJ, UK. E-mail: [neil.robertson@ed.ac.uk](mailto:neil.robertson@ed.ac.uk)

†Electronic supplementary information (ESI) available. CCDC 948496. For ESI and crystallographic data in CIF or other electronic format see DOI: 10.1039/c3dt51845k



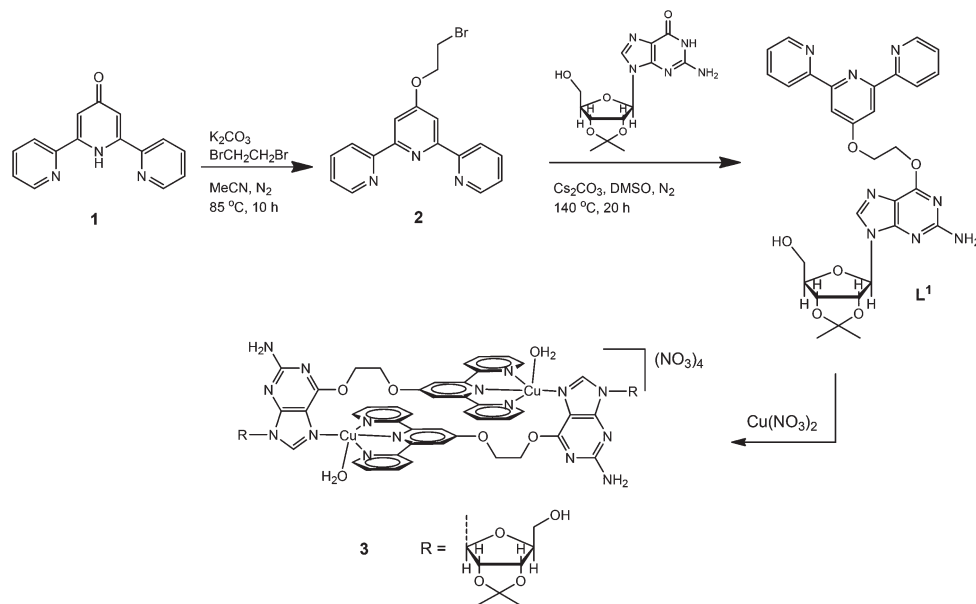


Fig. 1 Synthetic scheme for the preparation of ligand  $L^1$  and the di-copper(II) rectangle **3**.

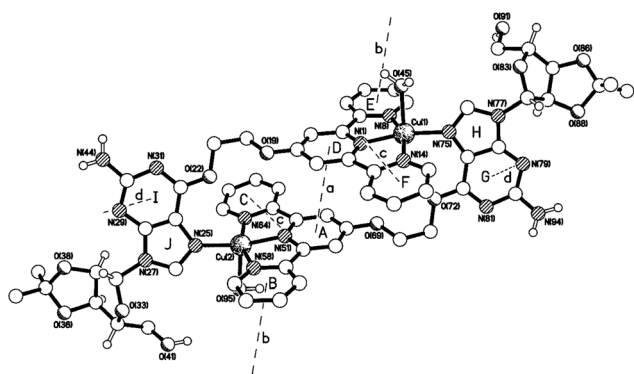


Fig. 2 The crystal structure of **3** showing the intra- and inter-molecular  $\pi$ - $\pi$  contacts (see Table 1 for details of distances).

terpyridine unit involved in a back-to-back intra-molecular  $\pi$ - $\pi$  stacking interaction (interaction a in Fig. 2, Table 1); the rectangle has approximate internal internuclear dimensions of 3.44 and 12.91 Å. The geometry at each copper centre is distorted square pyramidal with the water ligand occupying the apical site (see Table S1†). Adjacent molecules are linked by a series of  $\pi$ - $\pi$  contacts involving both the terpyridine (3.41 Å) and purine (3.33 Å) moieties to form an extended network.

Table 1 Intra- and inter-molecular  $\pi$ - $\pi$  contacts in the structure of **3**

Interaction	Rings	Centroid...centroid separation/Å	Mean interplanar separation/Å	Inclination between planes/°
a	A...D	3.81	3.41	1
b	B...E	3.87	3.41	2
c	C...F	3.75	3.37	2
d	G...I	3.76	3.33	7

Formation of rectangle **3** was further confirmed by ESI mass spectrometry which showed a small peak at 1510 a.m.u. assigned to  $[(Cu)_2(L^1)_2(NO_3)_3]^+$ . Several other peaks were observed consistent with the fragmentation of the  $[2 + 2]$  assembly under the mass spectrometric conditions (see Fig. S5† for spectrum). The UV-vis spectrum of **3** showed absorption bands at 334 nm, 323 nm and 280 nm as compared to the free ligand  $L^1$  at 281 nm. The molar extinction coefficient of **3** was determined to be  $24\,000\ M^{-1}\ cm^{-1}$  considering the absorption peak at 323 nm.

In order to study the magnetic properties of the di-copper(II) assembly, magnetic susceptibility measurements were carried out on a crystalline powder of **3** using a Quantum Design SQUID magnetometer. These measurements showed a linear response of magnetisation against field across 0–5000 Oe. The temperature dependence of the magnetic susceptibility was studied at an applied magnetic field of 1000 Oe in the temperature range 1.8–300 K. The  $1/\chi_M$  vs.  $T$  plot, fit in the temperature range 75–300 K, obeys the Curie-Weiss Law with a positive Weiss constant of  $\theta = 10.45\ K$  with  $C = 0.816\ cm^3\ mol^{-1}\ K$ , consistent with two copper(II) centres with  $g = 2.09$  (note:  $\chi_M T = 0.375\ cm^3\ mol^{-1}\ K$  for an  $S = 1/2$  ion with  $g = 2$ ). The plots of  $\chi_M$  vs.  $T$  and  $\chi_M T$  vs.  $T$  for two copper(II) ions are presented in Fig. 3. At room temperature  $\chi_M T = 0.84\ cm^3\ mol^{-1}\ K$ , is consistent to the Curie-Weiss fit. The  $\chi_M T$  value gradually increases upon decreasing the temperature from 300 K and reaches a maximum value of  $\chi_M T = 0.97\ cm^3\ mol^{-1}\ K$  at 47.68 K suggesting the presence of ferromagnetic interactions. On further cooling, it exhibits a rapid fall with  $\chi_M T = 0.86\ cm^3\ mol^{-1}\ K$  at 2 K. Although the magnetic data are likely influenced by several different interactions between centres leading to complex behaviour, the general rise of  $\chi_M T$  vs. with lower  $T$  and the positive  $\theta$  suggest a dominant ferromagnetic exchange between the copper(II) centres.



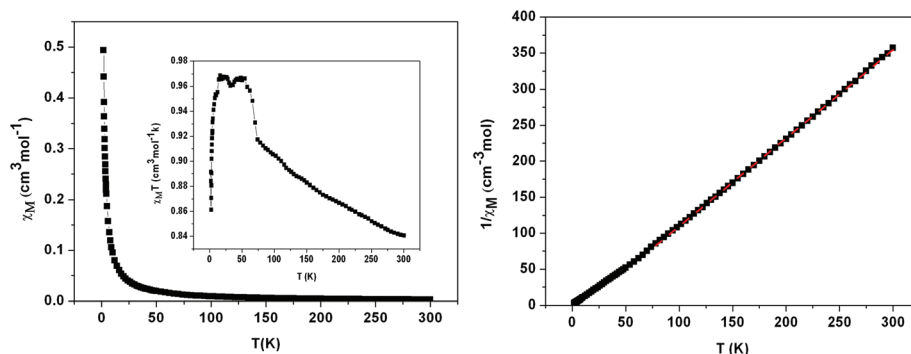


Fig. 3 Plot of  $\chi_M$  vs.  $T$  and  $\chi_M T$  vs.  $T$  (inset) (left) and plot of  $\chi_M^{-1}$  vs.  $T$  data fitting using Curie–Weiss equation in the range 80–300 K (right).

The X-ray crystal structure indicates that the two copper(II) centres are too far apart to show strong magnetic coupling through a superexchange mechanism. On the other hand, the crystal structure of **3** showed the presence of  $\pi$ – $\pi$  stacking interaction between the terpyridine moieties (with a mean interplanar separation of 3.41 Å – see Table 1). It has been previously reported that  $\pi$ – $\pi$  interactions can give rise to long-range ferromagnetic ordering between metal ions.<sup>17,22,23</sup> Therefore we propose that these inter-molecular interactions may serve as adequate superexchange mediators between the di-copper(II) centres and account for the observed ferromagnetic exchange.

In order to further study the interaction between the copper(II) cations in **3**, solution and solid state EPR studies were carried out. The EPR spectra of a frozen solution of **3** in DMSO at 5 K showed the characteristic quadruple splitting for copper(II) (Fig. S6†). The X-band EPR spectrum showed an axial signal with perpendicular component at  $g = 2.06$  and a shoulder derivative around  $g = 2.36$ . However, the coupling between the two copper centres in the molecule could not be detected by EPR due to the absence of a half field signal. The solid state Q band EPR spectra recorded at 4 K showed similar spectral features.

To investigate the potential coupling mechanism through inter- and/or intra-molecular  $\pi$ – $\pi$  contacts (a–d in Fig. 2 above) density functional theory (DFT) calculations were carried out on the model fragment systems 4–7 to simulate the relevant intra-molecular (4) and inter-molecular (5–7) interaction pathways (Fig. 4).

The system called for a sufficiently large basis set; the Ahlrichs' triple- $\zeta$  def2-TZVP basis set has been previously shown to be suitable for this type of system. Using the Broken Symmetry approach postulated by Noodleman *et al.*,<sup>24</sup> implemented in ORCA in conjunction with the popular UB3LYP functional coupling values of  $J_A = -4.47 \text{ cm}^{-1}$ ,  $J_B = -0.66 \text{ cm}^{-1}$ ,  $J_C = -0.08 \text{ cm}^{-1}$  and  $J_D = -0.61 \text{ cm}^{-1}$  were obtained. The interactions thus appear to be dominated by the intra-molecular  $\pi$ -stacking, with all of them calculated to be anti-ferromagnetic in nature. We note that the sign calculated for the magnetic exchange does not match the observation of a positive Weiss constant and rising  $\chi_{MT}$  value with decreasing temperature. Previously reported computational work on magnetic exchange through  $\pi$ -stacking and other non-bonding

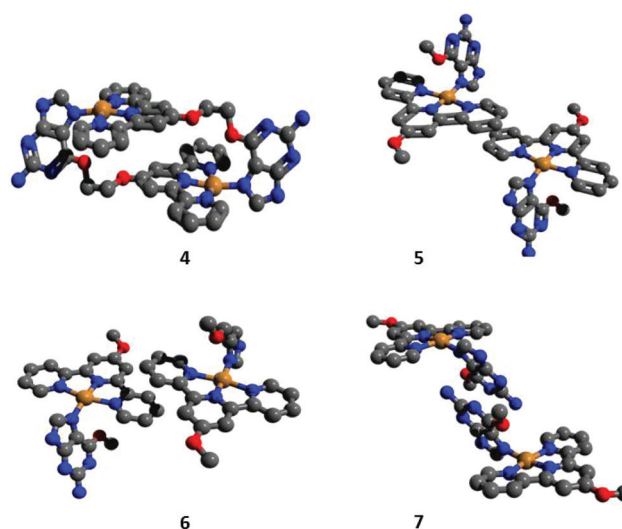


Fig. 4 Models 4–7 to represent  $\pi$ – $\pi$  stacking pathways a, b, c and d, respectively (hydrogens are omitted for clarity).

interactions, has also shown the quantitative relation between calculated and observed coupling constants to be limited.<sup>20</sup> In the case of **3**, where coupling constants are likely to be of a few wavenumbers, similar limits in the accuracy of the calculated  $J$  values may lead to determination of the opposite sign. The computational work, however, illustrates the spin density distribution and gives insight into the coupling mechanism. A closer look at the spin density reveals that it is indeed significantly lower than one on each of the Cu(II) centres (see Fig. S7 and Table S2†). Combined with the fact that the surrounding N atoms show spin contributions of the same sign, this indicates that the spin is delocalised from the metal 3d orbitals to the surrounding ligand atoms. As the magnetic coupling is accomplished through the  $\pi$ -stacking, the delocalisation is critical to propagate the coupling. A closer look at these data (Table S2†) reveals that most of the delocalised spin is located on the terpyridine ligand, in agreement with the larger magnitude of intra-molecular coupling value calculated. The McConnell spin-polarisation model<sup>25</sup> has previously been used to explain through-space couplings between overlapping aromatic fragments whereby regions of positive and negative spin



density on the respective fragments are aligned.<sup>26</sup> In the case of **3**, regions of positive spin density on one terpyridine ligand interact with regions of both positive and negative spin density on the other terpyridine (Fig. S7†) which is in keeping with the relatively low overall coupling constant observed.

In summary, herein we report a new self-assembled dicopper(II) rectangle which displays intra- and inter-molecular  $\pi$ - $\pi$  interactions. These play an important role in the ferromagnetic properties observed for this system showing that non-covalent interactions can be utilised to develop materials with interesting magnetic properties.

We thank the Royal Society for a Newton Research Fellowship (S.G.), the Engineering and Physical Sciences Council (EPSRC) for support and Dr Floriana Tuna from the EPSRC National EPR Research Facility and Service for the EPR data presented in this paper.

## Notes and references

†Crystal data for **3**: [C<sub>60</sub>H<sub>64</sub>Cu<sub>2</sub>N<sub>16</sub>O<sub>14</sub>](NO<sub>3</sub>)<sub>4</sub>·4MeOH·3H<sub>2</sub>O, *M* = 1790.61, triclinic, *P*1 (no. 1), *a* = 10.2878(3), *b* = 13.7254(5), *c* = 14.8599(5) Å,  $\alpha$  = 107.893(3),  $\beta$  = 103.008(3),  $\gamma$  = 94.397(3)°, *V* = 1921.34(12) Å<sup>3</sup>, *Z* = 1, *D*<sub>c</sub> = 1.548 g cm<sup>-3</sup>,  $\mu$ (Cu-K $\alpha$ ) = 1.574 mm<sup>-1</sup>, *T* = 173 K, blue tablets, Oxford Diffraction Xcalibur PX Ultra diffractometer; 9357 independent measured reflections (*R*<sub>int</sub> = 0.0272), *F*<sup>2</sup> refinement (G. M. Sheldrick, *Acta Crystallogr., Sect. A: Fundam. Crystallogr.*, 2008, **64**, 112–122). *R*<sub>1</sub>(obs) = 0.0495, *wR*<sub>2</sub>(all) = 0.1395, 8276 independent observed absorption-corrected reflections [*F*<sub>o</sub>] > 4 $\sigma$ (*F*<sub>o</sub>), 2 $\theta$ <sub>max</sub> = 145°, 1090 parameters. The absolute structure of **3** was determined by a combination of *R*-factor tests [*R*<sub>1</sub><sup>+</sup> = 0.0495, *R*<sub>1</sub><sup>-</sup> = 0.0512] and by use of the Flack parameter [*x*<sup>+</sup> = +0.05(4), *x*<sup>-</sup> = +0.95(4)]. CCDC 948496.

- R. Chakrabarty, P. S. Mukherjee and P. J. Stang, *Chem. Rev.*, 2011, **111**, 6810.
- Y.-R. Zheng and P. J. Stang, *J. Am. Chem. Soc.*, 2009, **131**, 3487.
- B. H. Northrop, A. Glockner and P. J. Stang, *J. Org. Chem.*, 2008, **73**, 1787.
- S.-S. Li, H.-J. Yan, L.-J. Wan, H.-B. Yang, B. H. Northrop and P. J. Stang, *J. Am. Chem. Soc.*, 2007, **129**, 9268.
- M. J. E. Resendiz, J. C. Noveron, H. Disteldorf, S. Fischer and P. J. Stang, *Org. Lett.*, 2004, **6**, 651.
- T. Murase, Y. Nishijima and M. Fujita, *J. Am. Chem. Soc.*, 2011, **134**, 162.
- M. D. Ward, *Chem. Commun.*, 2009, 4487.
- M. Yoshizawa, J. K. Klosterman and M. Fujita, *Angew. Chem., Int. Ed.*, 2009, **48**, 3418.
- J. E. Beves, B. A. Blight, C. J. Campbell, D. A. Leigh and R. T. McBurney, *Angew. Chem., Int. Ed.*, 2011, **50**, 9260.
- L. F. Lindoy, K.-M. Park and S. S. Lee, *Chem. Soc. Rev.*, 2013, **42**, 1713.
- Y. Inokuma, N. Kojima, T. Arai and M. Fujita, *J. Am. Chem. Soc.*, 2011, **133**, 19691.
- Y. Inokuma, M. Kawano and M. Fujita, *Nat. Chem.*, 2011, **3**, 349.
- T. Osuga, T. Murase, K. Ono, Y. Yamauchi and M. Fujita, *J. Am. Chem. Soc.*, 2010, **132**, 15553.
- Y. Yamauchi, Y. Hanaoka, M. Yoshizawa, M. Akita, T. Ichikawa, M. Yoshio, T. Kato and M. Fujita, *J. Am. Chem. Soc.*, 2010, **132**, 9555.
- K. Suzuki, K. Takao, S. Sato and M. Fujita, *J. Am. Chem. Soc.*, 2010, **132**, 2544.
- J.-M. Lehn, *Chem. Soc. Rev.*, 2007, **36**, 151.
- Y. H. Chi, L. Yu, J. M. Shi, Y. Q. Zhang, T. Q. Hu, G. Q. Zhang, W. Shi and P. Cheng, *Dalton Trans.*, 2011, **40**, 1453.
- D. Venegas-Yazigi, K. A. Brown, A. Vega, R. Calvo, C. Aliaga, R. C. Santana, R. Cardoso-Gil, R. Kniep, W. Schnelle and E. Spodine, *Inorg. Chem.*, 2011, **50**, 11461.
- K. Awaga, T. Tanaka, T. Shirai, M. Fujimori, Y. Suzuki, H. Yoshikawa and W. Fujita, *Bull. Chem. Soc. Jpn.*, 2006, **79**, 25.
- R. Perochon, P. Davidson, S. Rouziere, F. Camerel, L. Piekara-Sady, T. Guizouarn and M. Fourmigue, *J. Mater. Chem.*, 2011, **21**, 1416.
- C. M. Drain, J. D. Batteas, G. W. Flynn, T. Milic, N. Chi, D. G. Yablon and H. Sommers, *Proc. Natl. Acad. Sci. U. S. A.*, 2002, **99**, 6498.
- X. M. Ren, S. Nishihara, T. Akutagawa, S. Noro and T. Nakamura, *Inorg. Chem.*, 2006, **45**, 2229.
- D. Venegas-Yazigi, K. A. Brown, A. Vega, R. Calvo, C. Aliaga, R. C. Santana, R. Cardoso-Gil, R. Kniep, W. Schnelle and E. Spodine, *Inorg. Chem.*, 2011, **50**, 11461.
- L. Noodleman, *J. Chem. Phys.*, 1981, **74**, 5737.
- H. M. McConnell, *J. Chem. Phys.*, 1963, **39**, 1910.
- M. Viciano-Chumillas, N. Marino, I. Sorribes, C. Vicent, F. Lloret and M. Julve, *CrystEngComm*, 2010, **12**, 122.

